

Alternating Plane-View and Cross-Section Scanning Capacitance Microscope Technique to Reveal Various Implant Issue

Tsan-Chang Chuang, Cha-Ming Shen, Shi-Chen Lin, Chen-May Huang, Jin-Hong Chou, Jon C. Lee
Taiwan Semiconductor Manufacture Company, Ltd., Taiwan
1, Nan-Ke N, Rd., Tainan Science Park, Tainan, Taiwan 741-44, R.O.C.
Phone: 886-6-5056688 Ext. 7062149 Fax: 886-6-5052007 Email: Chuangtc@tsmc.com

INTRODUCTION

The International Technology Roadmap for Semiconductors identifies quantitative two-dimensional (2-D) and three-dimensional (3-D) dopant profiling as being essential for the advancement of future generations of the semiconductor technology [1]. Currently scanning capacitance microscopy (SCM) is a 2-D carrier and/or dopant concentration profiling technique under development that utilizes the excellent spatial resolution of scanning probe microscopy [2], [3]. It is based on the MOS characteristics between the scanning probe and the substrate and is regarded as having great potential for quantitative 2-D dopant concentration profiling [3], [4], and related framework diagram was shown as Fig-1.

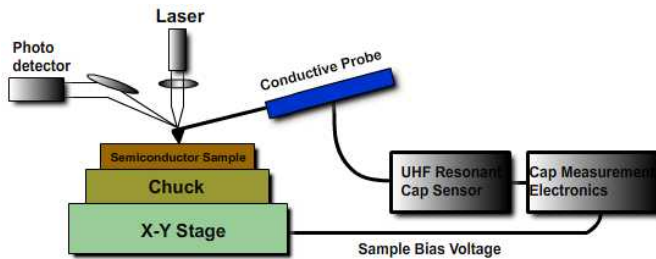


Fig-1: Scanning Capacitance Microscopy (SCM) framework Diagram with signal measurement and process unit.

As known to all, UHF resonant capacitance sensor is the basis of the capacitance detection. The resonator connects to a conductive probe via a transmission line. When the electrically resonating probe tip contacts a semiconductor, the sensor, the transmission line, probe and sample all become part of the resonator. Generally speaking, whole system is sensitive to variations as small as attofarads ($10^{-22} \text{ F}/\sqrt{\text{Hz}}$ sensitivity) [5]. And that is to say, majority-carrier depth that resonant capacitance sensor sensed is just ~ 4 lattice width. For failure analysis point of view, we need accurately localize defect position to near angstrom level for the purpose of making X-SCM analysis. Unfortunately, failure site localized indications such as, EMMI, OBIRCH, TIVA have insufficient capability to provide such precise position for X-SCM analysis especially at extensive zone. Besides, related to PV-SCM (Plane-View SCM), once the implant related defect was revealed by VC(voltage contrast), C-AFM(Conductive-Atomic Force Microscope) or NP (Nano-Probing), further

action has to take to confirm the failure mode. PV-SCM has limited capability to achieve the goal due to inherent "plane" trait. On top of that, deeper concentration profile just like DNW is also one of restrictions to use.

For representing above contents more clearly, the following cases would demonstrate the alternated and optimized application of PV-SCM and X-SCM.

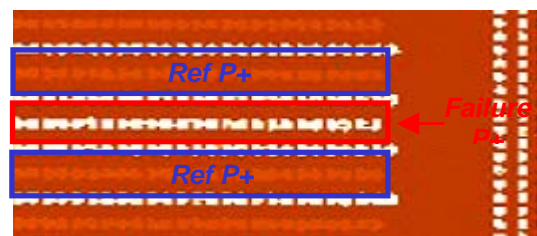
Case-1 Study: JTAG Failure

A new tape out product was suffered zero yield, 90% dies failed in JTAG (Joint Test Action Group) test. Then JTAG failure dice was picked for failure analysis, and a significant signal was detected at periphery circuit by IR-OBIRCH technique, as shown in Fig 2.

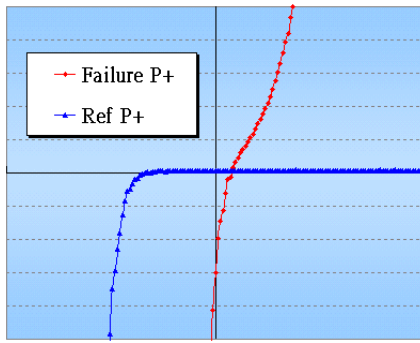


Figure 2: Dice with JTAG failure was detected a significant signal by IR-OBIRCH technique.

Brighter SEM PVC (passive voltage contrast) than normal was revealed, then current imaging and I-V curve using C-AFM were extracted, shown as Fig 3(a), (b) [6].



(a) C-AFM Current Imaging



(b) I-V curve measured by C-AFM

Figure 3: (a) Current imaging showed P+ column contacts suffered high reverse saturation leakage under the same OD with salicide process. (b) I-V curve measured by C-AFM showed smaller cut-in voltage and large reverse saturation current than reference for all leakage column P+ contacts.

Current imaging showed P+ column contacts suffered high reverse saturation leakage under the same OD with salicide process. I-V curve measured by C-AFM showed smaller cut-in voltage and large reverse saturation current than reference. Because the OBIRCH signal at huge protection diode area is wild enough, the follow up analysis is difficult to make judgment.

No physical abnormality could be found in this area even use wet chemical stain or TEM. The failure mechanism still not identified through conventional methods. X-SCM was chosen to make analysis and got nothing exceptional at localized wide site, shown as Fig 4.

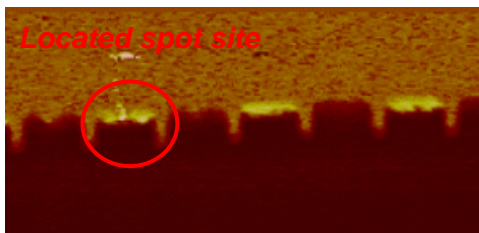


Figure 4: Although X-SCM technique was chosen to make analysis, SCM got nothing exceptional at localized site. That is to say, these kinds of defects couldn't be revealed by X-view.

Instead, for solving this issue, PV-SCM, shown as Fig 5, was applied to voyage at localized huge area and less P+ species per cubic was founded, shown as Fig 6.

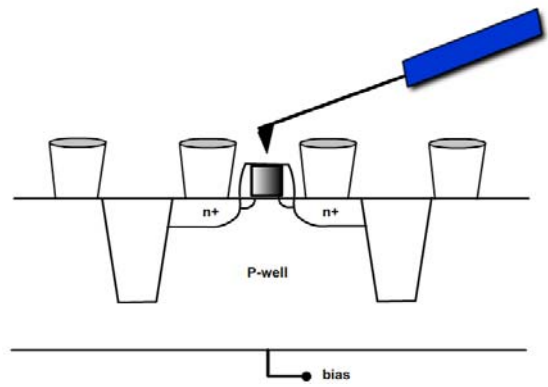
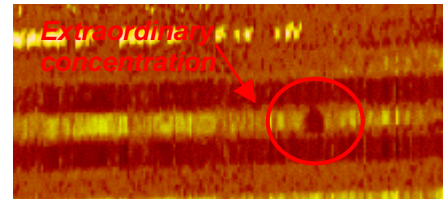
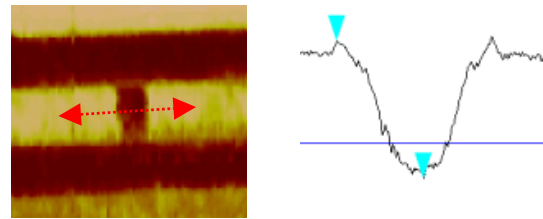


Fig-5: Sketch map showed the extraction of SCM imaging. Before SCM measurement started, an oxide re-grown over the sample.



(a) SCM mapping along the specific column of located P+/NW area



(b) Quantification analysis at revealed failure site

Figure 6: (a) An abnormality was revealed by SCM mapping along the specific row of located P+/NW area (b) The missed implantation issue was verified by the advanced quantification analysis of SCM signal at suspected spot.

Because failure dice has strong correlation with Fab in-line specific photo instrument, the failure mechanism should attribute to the weakness of related machine.

Case-2 Study: Stand-by Failure

From stand-by failure dice, A non-direct short between specific failed pins was revealed through electrical failure analysis, shown as Fig.7.

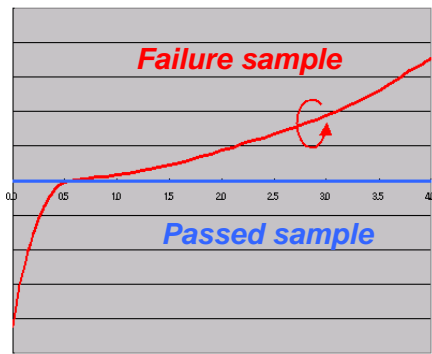


Figure 7: The failure die suffered stand-by failure was revealed a significant VDD to AVDD non-direct short phenomenon through electrical failure analysis.

The failure die was detected a significant signal by IR-OBIRCH technique and well leakage was suspected, as shown in Fig 8.

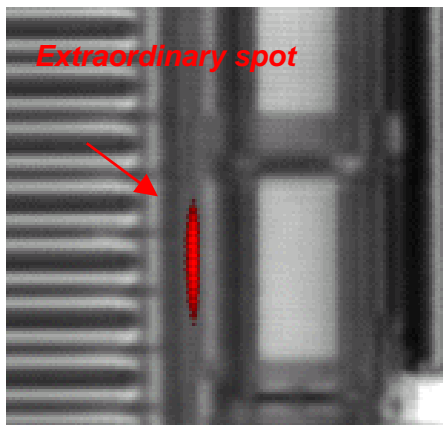
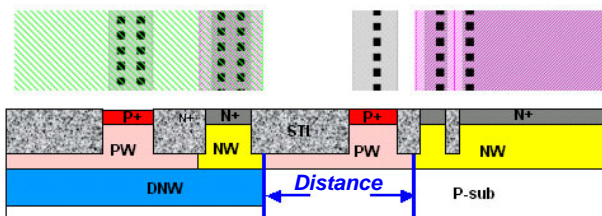
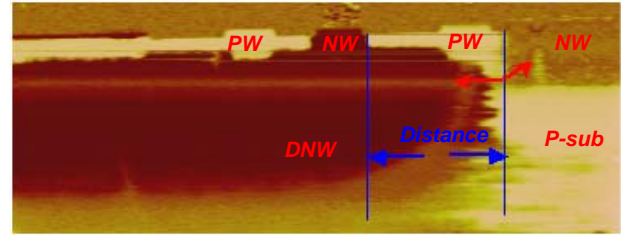


Figure 8: Momentous signal was detected at protection diode circuit region by IR-OBIRCH technique and well-to-well leakage was suspected.

No physical abnormality could be found in this area even using chemical stain, SEM layer-by-layer observation, FIB cross-sectional inspection or TEM analysis. The failure mechanism was still not identified through these methods. So SCM technique was chosen to make further analysis. According to our hypothesis, PV-SCM apparently lacks strength to do this kind of analysis due to deep-end area from si surface. X-SCM imaging was extracted, shown as Fig.9, and obviously DNW (Deep N-well) encroached to outside NW laterally was revealed.



(a) Layout and X-view



(b) X-SCM imaging

Figure 9: (a) Layout and X-view (b) Obviously DNW encroached to outside NW laterally was revealed. From the occurrence of isotropic extended DNW, it implied that excess thermal budget leading to such kind of non-direct short leakage.

Failure mode like that, isotropic extend of DNW, implied that excess thermal budget leading to such kind of non-direct short leakage should be the root cause.

Simulation also gave its approval for our inference. DNW with updated recipe showed less lateral diffusion due to lower thermal budget. Furthermore, related to DNW depth, SCM has about 25% difference between TCAD simulator and SCM technique, shown as Fig. 10.

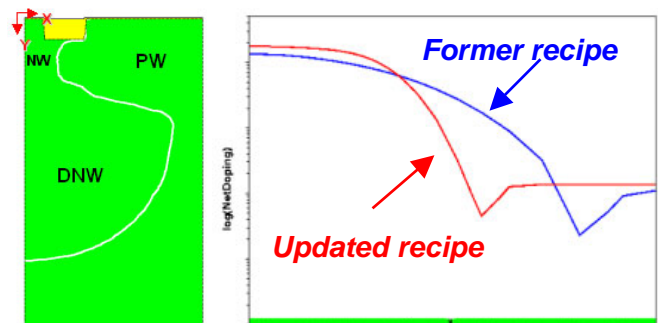


Figure 10: DNW with updated recipe showed less lateral diffusion due to lower thermal budget. Furthermore, related to DNW depth, SCM has about 25% difference between TCAD simulator and SCM technique.

CONCLUSIONS

These cases illustrates that correct selection from either plane-view or cross-sectional SCM analysis according to the surrounding of defect could help to exactly and rapidly diagnose the failure mechanism. X-SCM could make vertical profile analysis but it need precise defect position just like clockwork. PV-SCM could navigate at suspected area and efficiently reveal defect to reduce FA cycle time. But it could not provide deeper implant information due to the “plane” by birth. Alternating and optimizing PV-SCM and X-SCM techniques to navigate various implant issue could provide corrective actions that suit local circumstance of defects and identify the root cause.

REFERENCES

- [1] The International Technology Roadmap for Semiconductors, Semiconductor Industry Association, San Jose, CA, 2001, p. 16.
- [2] P. De Wolf, R. Stephenson, T. Trenkler, T. Clarysse, and T. Hantschel, "Status and review of two-dimensional carrier and dopant profiling using scanning probe microscopy," *J. Vac. Sci. Technol. B, Condens. Matter*, vol. 18, pp. 361–368, 2000.
- [3] A. C. Diebold, M. R. Kump, J. J. Kopanski, and D. G. Seiler, "Characterization of two-dimensional dopant profiles: Status and review," *J. Vac. Sci. Technol. B, Condens. Matter*, vol. 14, pp. 196–201, 1996.
- [4] C. C. Williams, "Two-dimensional dopant profiling by scanning capacitance microscopy," *Annu. Rev. Mater. Sci.*, vol. 29, pp. 471–504, 1999.
- [5] Application notes, Digital Instrument, Veeco Metrology Group.
- [6] Jone C Lee, C.H.Chen, David Su, J.H. Chuang, "Investigation of sensitivity improvement on Passive Voltage Contrast for Defect Isolation", ESREF processings (2002)